EMF Exposure of Human Head by Handset mmWave Phased Antenna Array

Zhekov, Stanislav Stefanov; Yao, Ming; Franek, Ondrej; Zhao, Kun; Zhang, Shuai

Published in:
16th European Conference on Antennas and Propagation, EuCAP 2022

DOI (link to publication from Publisher):
10.23919/EuCAP53622.2022.9769403

Publication date:
2022

Document Version
Accepted author manuscript, peer reviewed version

EMF Exposure of Human Head by Handset mmWave Phased Antenna Array

Stanislav Stefanov Zhekov, Ming Yao, Ondrej Franek, Kun Zhao, Shuai Zhang
Department of Electronic Systems, Technical Faculty of IT and Design, Aalborg University, Aalborg, Denmark
e-mail: stz@es.aau.dk; mingya@es.aau.dk; of@es.aau.dk; kz@es.aau.dk; sz@es.aau.dk

***Abstract*—Deployment of the fifth-generation (5G) mobile communications at the millimeter-wave (mmWave) part of the electromagnetic spectrum comes with concerns related to exposure of the human to electromagnetic field (EMF). The irradiation of the human body from phased antenna arrays, integrated into handsets operating at mmWave frequencies, is evaluated in terms of power density (PD). This paper presents a study on the local incident power density (IPD) on a surface made of vacuum and having the shape of the specific anthropomorphic mannequin (SAM) head phantom. The employed array consists of four off-ground half-wavelength dipoles. Two different orientations of the mobile terminal with respect to the phantom - cheek and tilt position are studied, as the goal is to find test exclusion possibilities. According to the results, the lower exposure in the tilt position (regardless of the frequency, inter-element spacing, and array excitation) allows tests for this handset orientation to be omitted.**

***Index Terms*—antenna array, dipole, exposure, handset, incident power density, mmWave.**

I. Introduction

The constantly increasing demand for higher data rates requires the use of larger frequency bandwidth. Part of the fifth-generation (5G) mobile communication systems are located at the millimeter-wave (mmWave) part of the spectrum [1] since a large amount of frequency resources is available there [2]. Due to the higher propagation loss at mmWave frequencies, high-gain phased antenna arrays need to be deployed in the handsets to increase the level of the signal [3]. The use of antenna arrays allows beam-steering, achieved by feeding the different radiating elements with different phases, increasing the spatial coverage [2].

Although the radio frequency (RF) electromagnetic field (EMF) exposure at the mmWave part of the spectrum is non-ionizing, it must be limited in order to prevent any adverse health effects and protect the human. The RF EMF safety guidelines have been published by regulatory authorities, such as U.S. Federal Communications Commission (FCC) [4], International Commission on Non-Ionizing Radiation Protection (ICNIRP) [5], and Institute of Electrical and Electronics Engineers (IEEE) [6]. At frequencies above 6 GHz, the safety guidelines for EMF exposure define the restrictions in terms of power density (PD). Currently, there are restrictions for local exposure imposed on both incident PD - IPD (reference level) and absorbed PD - APD (basic restriction). The two metrics need to be averaged as the restrictions are specified for averaging over 1 cm^2 and 4 cm^2 square. The RF EMF exposure restrictions set limits on the transmit power. On the other hand, the 3GPP specifies requirements on the range of effective isotropic radiated power (EIRP) and total radiated power (TRP) for UE [1]. The maximum transmit power by handset affects the radio coverage [7].

The relationship between skin temperature and averaged APD has been discussed in [8]–[10], while between surface skin temperature and averaged IPD in [8], [9]. A good correlation between the PD and the skin temperature has been observed. An estimation of APD in different human models from a four-element patch antenna array for different use scenarios has been presented in [11]. The ratio of the averaged APD to averaged IPD for various generic antennas, considering near- and far-field effects, has been quantified in [12]. The purpose has been to find a correlation between APD and IPD that can be used for compliance assessment of wireless devices based on free space measurements. Studies on the maximum EIRP which complies with the RF EMF exposure standards, in terms of averaged IPD have been shown in [3], [13], [14]. Investigations dealing with finding the size of the exposed volume (in terms of local IPD) around patch and dipole antenna arrays with different polarizations and inter-element distances have been presented in [15]. In the same work, finding the distance between two arrays to decouple their transmission has also been of interest.

The studies discussed above mainly focus on the analysis of the PD over a plane surface (exception is [11]). However, the human body, e.g. head, has a more complicated shape, and the distribution of PD on such a surface may show different properties. This paper presents a study on the IPD from handset dipole antenna array, placed at the bottom of the ground plane, for surface made of vacuum and having the shape of SAM head phantom. Due to the complicated shape of the surface of the human head, the local IPD is considered, rather than the averaged one. It should be mentioned that the averaging of APD in models (cylinder and sphere) with non-planar surfaces has been discussed in [16]. Two orientations of the mock-up with respect to the phantom are studied in this paper - cheek and tilt position. The motivation is to find test exclusion possibilities for handset with "bottom antenna array" as this has not been done before. That is, it is of interest to see whether tilt position can be excluded and thus to shorten the test time simply by limiting the number of studies. All investigations presented in the paper were conducted by using CST Microwave Studio 2019.

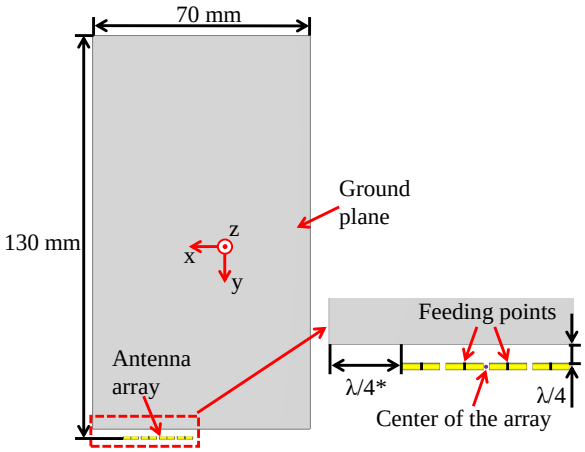

Fig. 1: Geometry of the antenna array and its placement with respect to the ground plane. Marking with asterisk (*) is used (see at the bottom left corner of the figure on the right-hand side) because the distance from the antenna array to the corner of the ground plane is $\lambda/4$ only when inter-element distance of 0.9λ is used.

II. Methodology for the Study of the Exposure

A. Power Density Calculation

The PD $|\vec{S}|$ is defined as time-averaged Poynting vector and calculated by:

$$|\vec{S}| = \frac{1}{2}|\mathrm{Re}[\vec{E} \times \vec{H}^*]| \tag{1}$$

where $\vec{E}$ and $\vec{H}$ are the complex electric and magnetic field vectors, respectively; (*) indicates complex conjugate. The results presented in the paper are obtained for 23 dBm (0.2 W) of radiated power as this is the maximum allowed radiated power for 5G UE [1]. This "power normalization" was performed by multiplying the simulated PD with 23 dBm and dividing this result by the simulated radiated power for each scenario (placement, frequency, inter-element spacing, and beam-forming precoding) separately. In this way, the effect of the total efficiency of the array in each scenario on the PD is removed and only the specifics in the radiation characteristics of the array in each scenario are considered.

Both ICNIRP [5] and IEEE [6] restrict the IPD averaged over 1 cm^2 and 4 cm^2 square, which should not exceed $55 f_{GHz}^{-0.177}$ and $110 f_{GHz}^{-0.177}$, respectively, where f_{GHz} is the frequency in GHz. In Canada, however, recommendation for human exposure limits are given by the expression $110 f_{GHz}^{-0.177}$, but for spatial local (non-averaged) peak IPD [18]. This allows us (since we investigate the local IPD) to use this recommendation to check whether the exposure found from our study is beyond the defined limit. In this paper, below 30 GHz, the frequency of 26 and 28 GHz are studied. Due to their proximity to 30 GHz, we will consider the expression defining the limit value valid for them. For all studied frequencies, one can find that the limit value for IPD is: 1) 61.8 W/m^2 at 26 GHz; 2) 61.0 W/m^2 at 28 GHz; and 3) 57.5 W/m^2 at 39 GHz.

B. Mock-up

A linear antenna array consisting of four half-wavelength dipoles was used in the study. The precise length of the dipoles was selected so that they have return loss better than 10 dB at the frequency of interest when one antenna is operating at the time. The antenna array is presented in Fig. 1; the same array was used in our previous study for finding an exposure volume [15]. The antennas are off-ground, i.e. they are placed beyond the ground plane. The reason to employ an off-ground antenna array is the fact that the on-ground antenna arrays have weak back radiation [15]. That is, the PD emitted by the on-ground antenna arrays towards the human head is low if the ground plane is located between the array and the head. Both antennas and ground plane were made of copper. In the simulation model, an air layer was used as a substrate (no dielectric loss).

Two different inter-element distances were studied: 0.5λ and 0.9λ, where λ is the free space wavelength at the corresponding frequency. The contour of the whole structure (antenna array and ground plane) has size a of 130 mm x 70 mm. The distance between the ground plane and the upper part of the antenna array in y-direction is $\lambda/4$; thus the electrical distance is kept the same among the studied frequencies. In order to keep the length of the entire structure to 130 mm, the length of the ground plane was trimmed accordingly at each studied frequency. The distance between the left-most antenna in the array and the left edge of the ground plane (x-direction) is $\lambda/4$ when inter-element distance of 0.9λ is used (this is marked with asterisk (*) in Fig. 1). However, the center of the array, no matter whether 0.5λ or 0.9λ is used, is kept the same.

C. Varied Parameters in the Study

For the sake of obtaining more thorough information about the IPD on human head and finding the worst-case scenario, the following variables were employed in the study:

- inter-element distance: 0.5λ and 0.9λ.
- frequency: 26 GHz, 28 GHz, and 39 GHz.
- beam-forming precoding - the IPD was evaluated for different excitations of the array elements. More precisely, the magnitude of the signals feeding the array elements was kept 1 (all array elements were fed with signals with the same magnitude), but the phase of these signals was progressively changed from one antenna element to the next antenna element. This can be written as feeding the array elements with $w_i = [1, 1e^{-j\phi}, 1e^{-j2\phi}, 1e^{-j3\phi}]$, where the subscript i varies between 1 and 4 indicating the antenna element ($w_1 = 1$, $w_2 = 1e^{-j\phi}$, etc.), the phase ϕ takes values of $0°, \pm 30°, \pm 60°, \pm 90°, \pm 120°$. That is, beam steering with phase shifts between elements: $0°, +30°, +60°, +90°, +120°, -30°, -60°, -90°, -120°$ was used.
- two different placements of the mock-up with respect to the phantom: 1) cheek position (Fig. 2(a)); and 2) tilt position (Fig. 2(b)). The side view for the touch position

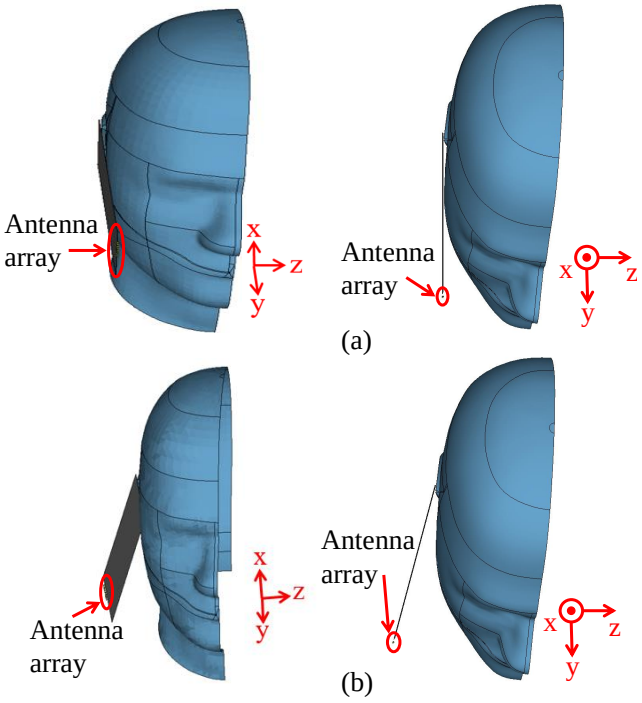

Fig. 2: Front (left-hand side) and top (right-hand side) view of the antenna array and a vacuum surface with the shape of SAM head phantom: (a) cheek position, and (b) tilt position.

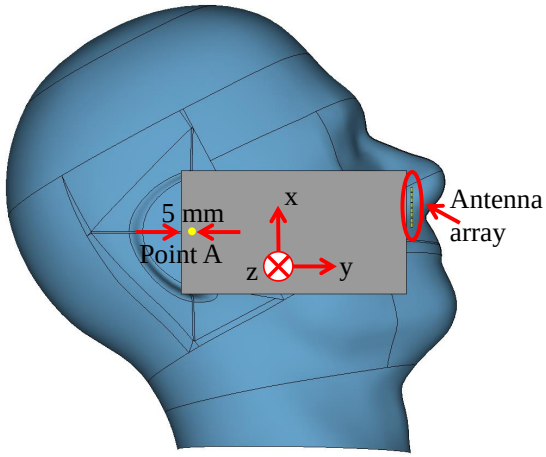

Fig. 3: Side view of the antenna array and a vacuum surface with the shape of SAM head phantom.

is given in Fig. 3. The placement of the mock-up in both scenarios is as defined in [17]. The distance from the edge of the ground plane to "point A" (being an imaginary audio output) is selected 5 mm. This location of the antenna array (at the bottom corner of the structure) is selected, because it is considered to be the most realistic one. The latter is in case that there is an antenna array in 5G handset and this array is used in talk mode.

The reason for studying two different mock-up orientations, as mentioned above, was to check whether the tilt scenario can be excluded from exposure tests. The exclusion of this case means that less measurement will need to be conducted, which will speed up the test process.

III. Results

Due to the shape of the surface of the human head, respectively of the SAM phantom, the normal component of the PD to that surface does not match exactly with either of the x-, y-, or z-components; the normal component is rather defined by some combination between S_x, S_y, and S_z. To each infinitesimally small area different normal vector would need to be found (and then to evaluate the value of the normal component of the PD) which is a difficult task. Because of the complicated shape, as a metric for comparing the exposure of the head phantom between different study cases can be used the norm $||S||$ of the PD since it is direction independent parameter. Evaluating the norm is simple and it presents the most conservative scenario (although in the classical far-field exposure case the normal component is of interest; the norm has been of interest in [12]) and can serve as an upper limit.

TABLE I: Peak value of the local IPD for cheek/tilt position and the progressive phase shift between the array antennas leading to the highest exposure for 0.5λ inter-element spacing.

Power density component	Frequency (GHz)	Cheek/tilt position	
		Peak value (W/m^2)	Phase shift (°)
$\|S_x\|$	26	24.8/6.8	120/90
	28	24.5/7.2	120/120
	39	22.6/7.1	120/120
$\|S_y\|$	26	22.1/5.7	30/30
	28	22.2/5.6	30/30
	39	21.1/5.3	30/30
$\|S_z\|$	26	41.0/16.1	60/30
	28	39.1/15.8	60/60
	39	35.5/14.4	60/30
$\|\|S\|\|$	26	45.5/16.6	60/60
	28	44.0/16.6	60/60
	39	40.7/15.2	60/60

TABLE II: Peak value of the local IPD for cheek/tilt position and the progressive phase shift between the array antennas leading to the highest exposure for 0.9λ inter-element spacing.

Power density component	Frequency (GHz)	Cheek/tilt position	
		Peak value (W/m^2)	Phase shift (°)
$\|S_x\|$	26	10.9/5.4	120/120
	28	11.6/5.6	120/120
	39	12.9/6.0	120/120
$\|S_y\|$	26	14.1/6.4	30/30
	28	16.7/6.3	30/30
	39	22.5/7.2	30/30
$\|S_z\|$	26	35.0/19.7	0/30
	28	37.9/19.7	0/30
	39	44.7/20.2	0/60
$\|\|S\|\|$	26	35.3/20.0	30/30
	28	37.9/20.2	0/60
	39	45.0/21.0	30/60

The distribution of the norm of the local IPD on the vacuum surface at 28 GHz for progressive phase shifts of 0°, $-120°$, and 120°, for cheek position and tilt position, for 0.5λ is presented in Fig. 4 and for 0.9λ in Fig. 5. As expected, the

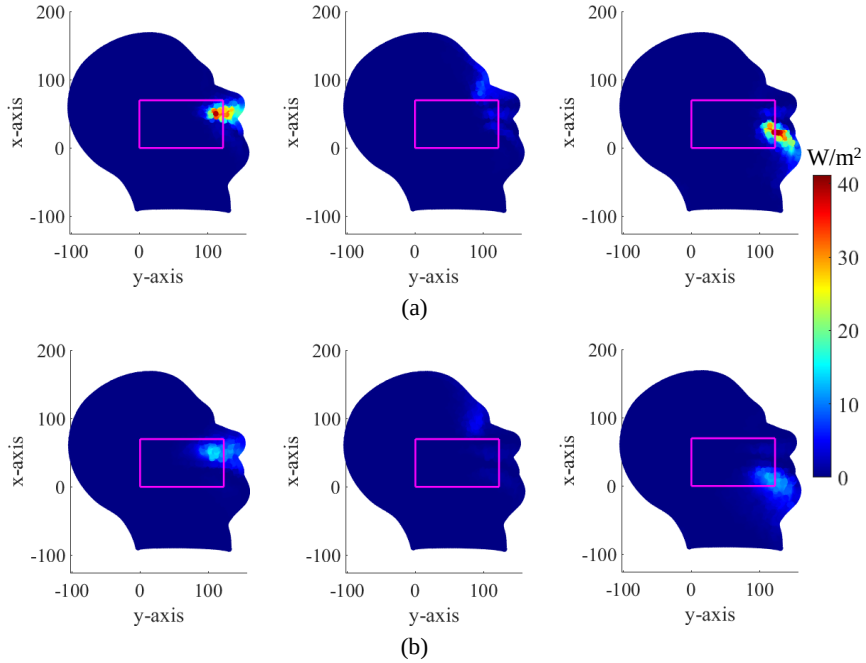

Fig. 4: Distribution of the norm of the local IPD on a vacuum surface with the shape of SAM head phantom at 28 GHz for 0.5λ inter-element spacing for: (a) cheek, and (b) tilt position. The results on the left-hand side are for 0°, in the center for -120°, and on the right-hand side for 120° progressive phase shift between the array elements. With purple is presented the contour around the entire structure (antenna array + ground plane).

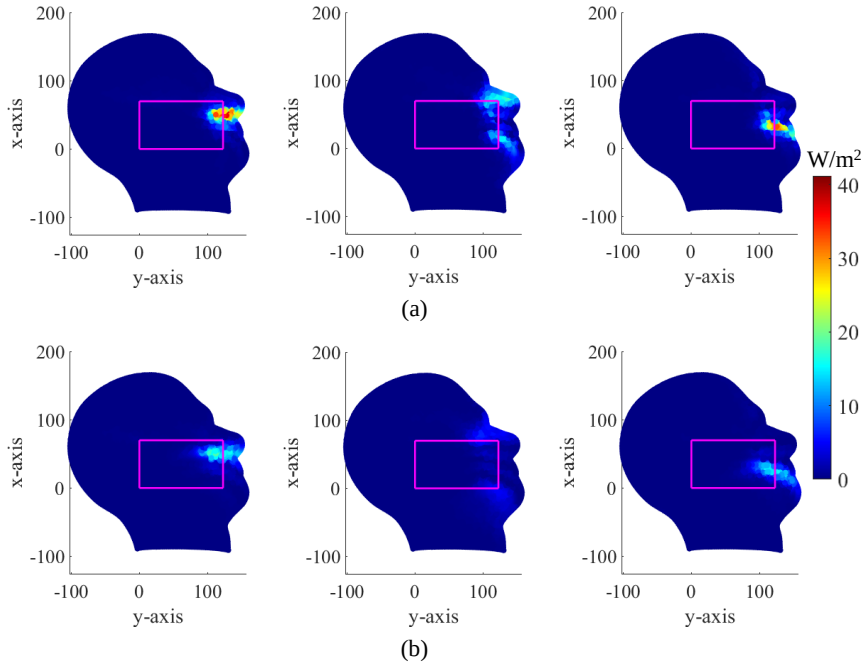

Fig. 5: Distribution of the norm of the local IPD on a vacuum surface with the shape of SAM head phantom at 28 GHz for 0.9λ inter-element spacing for: (a) cheek, and (b) tilt position. The results on the left-hand side are for 0°, in the center for -120°, and on the right-hand side for 120° progressive phase shift between the array elements. With purple is presented the contour around the entire structure (antenna array + ground plane).

beam-steering leads to spatial shift in the position (and the value) of the peak of the IPD. The IPD is significantly higher in cheek than in tilt position.

The peak IPD found among all studied beam-forming precoding combinations is given in Table I for 0.5λ and in Table II for 0.9λ inter-element distance. For completeness,

the results for all components and norm are presented in the tables. It should be kept in mind that the values, in each single scenario, are normalized as in this way the effect of the total efficiency is removed; the findings discussed below are therefore valid for the case when normalization is performed. The obtained peak IPDs are below the exposure limits: 1) 61.8 W/m^2 at 26 GHz; 2) 61.0 W/m^2 at 28 GHz; and 3) 57.5 W/m^2 at 39 GHz. As already mentioned, the IPD is higher in the cheek than in the tilt position. Therefore, the tilt position might be excluded from exposure tests; however, more studies of various array designs might be needed to confirm this completely. The results at 26 and 28 GHz (since they are relatively close to each other) differ only slightly. The strongest exposure is observed at 26 or 28 GHz (depending on which component is considered) for 0.5λ inter-element spacing and at 39 GHz for 0.9λ inter-element spacing. The peak of all components and the norm of the IPD in cheek position is higher for 0.5λ inter-element spacing than for 0.9λ at 26 and 28 GHz, but not for $|S_y|$, $|S_z|$, and $||S||$ at 39 GHz. The peak $|S_y|$, $|S_z|$, and $||S||$ in tilt position is higher for 0.9λ inter-element spacing than for 0.5λ at the three studied frequencies. The peak IPD for $|S_y|$, $|S_z|$, and $||S||$ appears for relatively small progressive phase shifts - between 0° and 60°. The difference between the peak $|S_z|$ and $||S||$ (although they might appear for different phase shifts) is smaller compared to that between any of the other two components and the norm. The largest component is $|S_z|$ and it contributes the most to the value of the norm in the region with the strongest exposure.

IV. Conclusion

A study on the local IPD for a surface made of vacuum with the shape of SAM phantom has been presented in this paper. An off-ground antenna array containing four dipoles was used as a radiator. For this type of antenna array, the exposure is stronger at 26 or 28 GHz than at 39 GHz for 0.5λ inter-element spacing, and stronger at 39 GHz than at 26 or 28 GHz for 0.9λ inter-element spacing. Due to the complicated shape of the human head, it is difficult to find the normal vector to the surface for each infinitesimally small area. However, for the studied antenna array and orientation, the peak value of the z-component is the closest one to the peak value of the norm of the IPD. The norm of the Poynting vector is the most conservative metric. The strongest exposure is observed for phase shifts in the range 0° - 60°, but for other phases values close to the peak one can also be observed. The exposure found among all studied cases is below the limit - the highest z-component of the PD is 44.7 W/m^2 for cheek and 20.2 for tilt position, and norm is 45.5 W/m^2 for cheek and 21.0 for tilt position. These values are below the limit ones.

The exposure in the cheek position is stronger than that in the tilt position for this antenna configuration. Therefore, testing only in cheek position might be enough for estimating the exposure, and thus test reduction can be achieved.

Acknowledgment

The authors would like to thank K. H. Joyner at Mobile and Wireless Forum, Kai Niskala at Samsung Electronics Co. Ltd., B. Xu and D. Colombi at Ericsson AB, and Z. Ying at Sony Corporation for helpful discussion.

References

[1] *User Equipment (UE) radio transmission and reception; Part 2: Range 2 Standalone,* Technical specification (TS) 38.101-2, 3GPP, Rev. 16.0.0, Jun. 2019.

[2] W. Hong, K.-H. Baek, Y. Lee, Y. Kim, and S.-T. Ko, "Study and prototyping of practically large-scale mmWave antenna systems for 5G cellular devices," *IEEE Commun. Mag.*, vol. 52, no. 9, pp. 63-69, Sept. 2014.

[3] W. He, B. Xu, Y. Yao, D. Colombi, Z. Ying, and S. He, "Implications of incident power density limits on power and EIRP levels of 5G millimeter-wave user equipment," *IEEE Access*, vol. 8, pp. 148214-148225, 2020.

[4] *Radiofrequency radiation exposure limits*, FCC, Washington, DC, USA, 2013.

[5] International commission on non-ionizing radiation protection (ICNIRP), "Guidelines for limiting exposure to electromagnetic fields (100 kHz to 300 GHz)," *Health Phys.*, vol. 118, no. 5, pp. 483–524, May 2020.

[6] *IEEE standard for safety levels with respect to human exposure to electric, magnetic, and electromagnetic fields, 0 Hz to 300 GHz*, Standard C95.1-2019, 2019.

[7] S. S. Zhekov and G. F. Pedersen, "Over-the-air evaluation of the antenna performance of popular mobile phones," *IEEE Access*, vol. 7, pp. 123195-123201, 2019.

[8] K. Li, K. Sasaki, S. Watanabe, and H. Shirai, "Relationship between power density and surface temperature elevation for human skin exposure to electromagnetic waves with oblique incidence angle from 6 GHz to 1 THz," *Phys. Med. Biol.*, vol. 64, no. 6, 2019.

[9] A. Hirata, D. Funahashi, and S. Kodera, "Setting exposure guidelines and product safety standards for radio-frequency exposure at frequencies above 6 GHz: brief review," *Ann. Telecommun.*, vol. 74, pp. 17–24, 2019.

[10] T. Nakae, D. Funahashi, J. Higashiyama, T. Onishi, and A. Hirata, "Skin temperature elevation for incident power densities from dipole arrays at 28 GHz," *IEEE Access*, vol. 8, pp. 26863-26871, 2020.

[11] M. S. Morelli, S. Gallucci, B. Siervo, V. Hartwig, W. He, and S. He, "Numerical analysis of electromagnetic field exposure from 5G mobile communications at 28 GHz in adults and children users for real-world exposure scenarios," *Int. J. Environ. Res. Public Health*, vol. 18, no. 3, Jan. 2021.

[12] A. Christ, T. Samaras, E. Neufeld, and N. Kuster, "Limitations of incident power density as a proxy for induced electromagnetic fields," *Bioelectromagnetics*, vol. 41, no. 5, pp. 348-359, 2020.

[13] B. Thors, D. Colombi, Z. Ying, T. Bolin, and C. Tornevik, "Exposure to RF EMF from array antennas in 5G mobile communication equipment," *IEEE Access*, vol. 4, pp. 7469–7478, 2016.

[14] B. Xu, K. Zhao, Z. Ying, D. Sjöberg, W. He, and S. He, "Analysis of impacts of expected RF EMF exposure restrictions on peak EIRP of 5G user equipment at 28 GHz and 39 GHz bands," *IEEE Access*, vol. 7, pp. 20996–21005, 2019.

[15] S. S. Zhekov, K. Zhao, O. Franek, and S. Zhang, "Test reduction for power density emitted by handset mmWave antenna arrays," *IEEE Access*, vol. 9, pp. 23127-23138, 2021.

[16] Y. Diao, E. A. Rashed, and A. Hirata, "Assessment of absorbed power density and temperature rise for nonplanar body model under electromagnetic exposure above 6 GHz," *Phys. Med. Biol.*, vol. 65, no. 22, 2020.

[17] *Measurement procedure for the assessment of specific absorption rate of human exposure to radio frequency fields from hand-held and body-mounted wireless communication devices - Part 1: Devices used next to the ear (Frequency range of 300 MHz to 6 GHz)*, Standard IEC 62209-1:2016, IEC, Rev. 2.0, July 2016.

[18] *Localized human exposure limits for radiofrequency fields in the range of 6 GHz to 300 GHz*, Health Canada, Jan. 2021.